Self-Induced Cyclic Reorganization of Many Bodies Through Thermal Convection

Bin Liu[1] and Jun Zhang[1,2*]
[1] *Center for Soft Matter Research, Department of Physics, New York University, 4 Washington Place, New York, NY 10003, USA*
[2] *Applied Mathematics Laboratory, Courant Institute, New York University, 251 Mercer Street, New York, NY 10012, USA*

We investigate the dynamics of a thermally convecting fluid as it interacts with freely moving solid objects. This is a previously unexplored paradigm of many-body interactions mediated by thermal convection, which gives rise to surprising robust oscillations between different large-scale circulations. Once begun, this process repeats cyclically, with the collection of spheres entrained and packed from one side of the convection cell to the other. The frequency of the cycle is highest when the spheres occupy about half of the cell bottom and their size coincides with the thickness of the thermal boundary layer. This phenomenon shows that a deformable mass can stimulate a turbulent, thermally convecting fluid into oscillation, a collective behavior that may be found in nature.

PACS numbers: 47.27.te, 47.20.Bp, 05.65.+b

A fluid, when heated from below and cooled at the top, is subject to buoyancy instability; subsequently, Rayleigh-Bénard convection arises as the warmer fluid ascends and the cooler fluid descends. A large-scale circulation of the bulk fluid emerges from the turbulent flow as the system exceeds a finite threshold of external forcing [1–7]. The forcing intensity is characterized by the dimensionless Rayleigh number [8], $\mathrm{Ra} = \alpha g \Delta T H^3/\nu\kappa$, where g is the acceleration due to gravity, ΔT is the temperature difference between bottom and top, H is the depth of the fluid, and α, κ and ν are the thermal expansion coefficient, the thermal diffusivity, and the kinematic viscosity of the fluid, respectively. The threshold Rayleigh number for a large-scale flow to appear is on the order of 10^7 [2, 9]. At the top and the bottom plates, thin thermal boundary layers exist, within which convection is suppressed by the no-slip condition at the fixed boundaries. Within these regions, thermal conduction alone provides the vertical heat transfer. The thickness of the thermal boundary layer λ_{th} is observed to have different scaling dependencies on the Rayleigh and Prandtl numbers ($\mathrm{Pr} = \nu/\kappa$) in various regimes, as summarized by Grossmann and Lohse [10, 11]. In the regime of our experiment, $\mathrm{Ra} \sim 10^{8-9}$ and $1 < \mathrm{Pr} < 10^2$, the scaling relationship is given by the measurement of Ashkenazi and Steinberg [12], $\lambda_{\mathrm{th}}/H = 2.3\mathrm{Ra}^{-0.3}\mathrm{Pr}^{0.2}$.

Turbulent thermal convection has been one of the most studied physical dynamical processes in recent decades [13, 14]. Its study has revealed fundamental and generic features of systems driven from equilibrium and into chaos [15, 16], and many open questions still remain, especially on the heat transport at high Rayleigh numbers [11, 17, 18] and on the dynamical stability of the large-scale circulation [19, 20]. However, most experimental and theoretical studies of thermal convection have dealt with fixed boundary conditions: all the solid walls are rigid, and they do not respond to or interact with the fluid flows confined within. Previous experiments[21–24], meant to simulate a continent drifting over mantle convection, have shown coupled motion of a single floating boundary interacting with the fluid underneath. The experiment discussed here aims to investigate the interac-

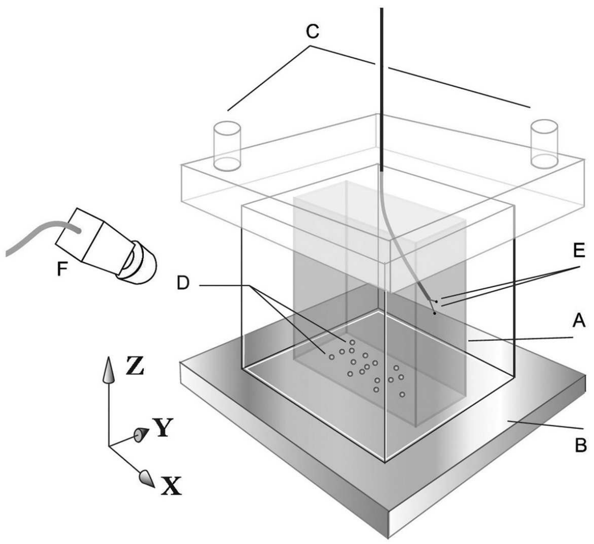

FIG. 1: The experimental setup. A thermal convection cell (A), shown in gray, is surrounded by another box that contains the same fluid and subject to the same cooling (C) and heating (B), so that the inner convection cell is well insulated at all vertical walls. Nylon spheres (D) are able to roll freely on the smooth, mirror-quality bottom as they are entrained by the convecting fluid. The system we study consists of the inner convection cell and the enclosed spheres. A pair of vertically separated thermistors (E) measures the bulk temperature, and flow velocity through the cross-correlation between the two signals. Conformal transformation of the images taken by a video camera (F), produces top-viewed spheres patterns.

tion between a collection of many bodies – on the order of a few hundreds – and the surrounding convective fluid.

As shown in Fig. 1, a Rayleigh-Bénard convection cell of $20 \times 18.4 \times 7.6$ cm ($H \times L \times W$), containing a water-glycerol mixture ($\rho = 1.115$ g/ml), is heated from below by a DC electric heater and cooled at its top with a water circulator. The relatively smaller width (W) of the cell allows only two possible large-scale circulations to exist at high Rayleigh numbers (Ra $> 10^7$): a clockwise circulation or counter-clockwise one (from the perspective of the camera) that occupies the entire cell. To eliminate lateral heat exchange through the side walls, this convection cell is contained within a bigger box which holds the same fluid and subject to the same cooling and heating.

The freely moving objects introduced into the inner convection cell are nylon spheres, which are a few millimeters in diameter (d) and 2% denser ($\rho' = 1.134 \pm 0.002$ g/cm^3) than the fluid. A large number of the spheres – N, on the order of a few hundreds – form a single loose layer at the bottom. They can move along the mirror-quality bottom as each sphere experiences fluid drag from the convective flow. The typical Stokesian drag force, $F_{\rm drag} \sim 6\pi\eta dU$, is on the order of a few hundredth of a dyne, given the sphere size, the speed of the convecting flow, U, and its viscosity, η.

In the absence of the spheres, either the clockwise or the counter-clockwise large-scale circulation is stable up to a time-scale of around 40 hours. Beyond this time-scale, the circulation can flip direction spontaneously in a random fashion. This is consistent with observations made earlier in a cylindrical cell as the relative rare cessation events took place [19, 20], and such flow reversals are regarded as a result of hydrodynamical fluctuations overcoming a potential barrier that separates the possible states [25].

Having added the spheres to the convection cell, however, we find a drastic acceleration of these flow reversal events. Driven by the reversing circulation, the spheres are packed and unpacked cyclically. Figure 2 shows a sequence of sphere positions during this process. Under large-scale circulation, the spheres are entrained by the flow and packed at one end of the cell bottom (Figs. 2a and 2c). This aggregation is made progressively, often one sphere at a time or with small clusters, by the flow that travels across the bottom. Typical packing patterns include thin strips of square lattice aligned with the side-walls and small patches of triangular patterns near the interior of the pack. These patches are pieced together in a random fashion as they evolve in time.

As the flow reverses direction, the spheres become unpacked (Figs. 2b, 2d). Figures 3a and 3b show that unpacking of the aggregate starts soon after the circulation reverses direction. Shown in Fig. 2e, flow reversal happens only after the majority of spheres have collected on one side. Even though these flow reversals take place with varying degree of randomness, depending on each

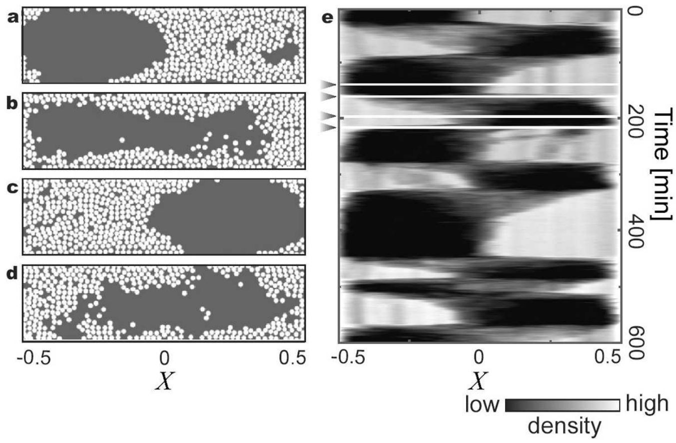

FIG. 2: Interaction between 426 spheres of diameter 3.2 mm and the convective fluid at Ra $= 3.2 \times 10^9$. (a-d): four successive snapshots of the spheres during one cycle of two adjacent reversals. Two instances (a and c) show relatively dense packing, and two others (b, d) show the transient period as the aggregate is unpacked. Each of the snapshot is averaged along the short side of the convection cell to obtain a one-dimensional density profile. The evolution of such a profile (e) demonstrates cyclic packing and unpacking of the mobile spheres, while the four horizontal lines indicating the four instances shown on the left.

experimental condition (Ra and N), an average reversal interval can be well-defined.

The migration of an individual sphere takes up to a few tens of seconds, which is 2 - 5 times the duration needed for the circulation to flow across the bottom. However, it can take considerable time for a dense packing to assemble. Jamming of spheres during the packing phase often yields vacancies (e.g.: the one seen near the right end of Fig 2a). The extent and location of these vacancies fluctuate in time and they are likely to be filled before the next reversal. It is conceivable that the randomness in the process of achieving dense packing is the main source of randomness in the timing of flow reversal.

The longest time-scale in the oscillation is apparently that between flow reversals. Once the circulation changes direction, it achieves its full strength in a much shorter time-scale, typically within a few flow circulations (Fig. 3a). Due to the coupling between the thermally convective flows and the free-moving spheres, relatively stable large-scale circulations are interrupted by abrupt flow reversal events and followed by the slow and accumulative aggregation of free-moving bodies. Figure 3b shows the correlation between the flow velocity and the position of the aggregate as a whole.

The spheres play an important role in inducing the circulation to reverse, and they collectively cause the coupled system to oscillate. The frequency of the self-sustained oscillation depends on the effectiveness of the perturbation introduced by the spheres. Figure 3c illus-

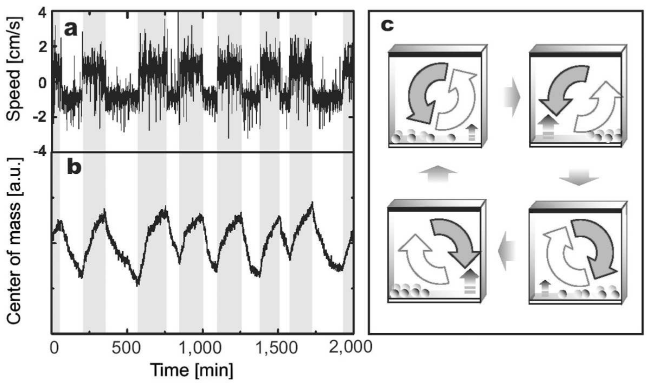

FIG. 3: Correlation between the large-scale circulation and the collection of the spheres. Here, $N = 510$, $d = 3.2$ mm and $\mathrm{Ra} = 1.8 \times 10^9$. Graph (a) shows a time series of the circulation velocity, switching in time between two circulatory states. Graph (b) indicates that the center of mass of all spheres varies in phase with the clockwise circulation (white bands) and the counter-clockwise circulation (grey bands). Illustration (c) shows the interaction between the large-scale circulation and the spheres. Once packed, the spheres collectively counteract the circulation by suppressing the local heat flux (relatively strong heat flux shown as vertical arrow). The large-scale flow eventually reverses its direction. The new circulation unpacks the spheres and drives them to the other side of the convection cell, where they are reassembled. Once initiated, this process repeats cyclically.

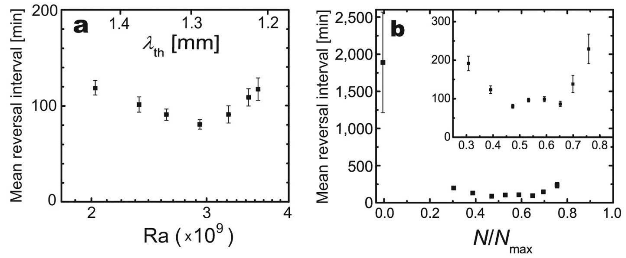

FIG. 4: The Rayleigh number and the number of free spheres are varied. (a) The circulation reversal intervals as a function of the Rayleigh number when $d = 3.2$ mm and $N = 365$. An oscillation with shortest reversal interval is obtained when the thickness of the thermal boundary layer, λ_{th}, is comparable to the radius ($d/2$) of the spheres. (b) At $\mathrm{Ra} = 3.1 \times 10^9$ and $d = 3.2$ mm, the dependence of the reversal interval on the number of spheres. $N_{\max}$ (~ 840) is the number of spheres needed to fill up the bottom with random packing [29]. The inset shows the zoom-in detail of the data at $N \sim N_{\max}/2$.

trates the feedback mechanism that is likely to operate in our coupled solid-fluid system. In our earlier work, we have shown that a solid boundary of similar material and thickness reduces the local heat transfer by a factor of order 10, because it prohibits local convective heat transfer [22, 24]. This effect is similar to the thermal blanketing effect of a solid boundary studied in geophysical contexts [26, 27]. In the current experiment, the precise heat-transfer contrast between a sphere-packed area and an unpacked area depends on the detailed packing configuration. For a typical random packing, we estimate that such contrast is on the order of 3 - 5, based on the volume occupied by the spheres compared with a solid block. Collectively, the aggregate of spheres act as a thermal blanket that reduces the local heat flux from the bottom plate; it relatively enhances local heat influx at the unoccupied areas. This contrast eventually overturns the existing large-scale circulation and cyclic oscillations thus emerge.

To modify the amplitude and nature of the perturbation to the system, we use different sizes of spheres, vary the coverage ratio by adjusting the number of spheres, and also vary the Rayleigh number. As we change the boundary layer thickness by varying the Rayleigh number while using the same group of spheres, we find that there is a minimal flow reversal interval when $\lambda_{\mathrm{th}} \sim d/2$, as shown in Fig. 4a. We conjecture that the thermal blanketing effect of an individual sphere is affected by its area fraction at a height h from the bottom (the cross-section area at height h normalized by its maximum cross-section at height $d/2$), which is $\Gamma = 4(d-h)h/d^2$, where $h < d$. When $h = d/2$, this expression takes its maximum value. Our observation hence suggests that when the sphere radius ($d/2$) is close to λ_{th}, the activity at the edge of the thermal boundary layer – the most active region in a thermally convecting fluid [28] – is most efficiently suppressed.

We notice that the radius of the spheres ($d/2 = 1.6$ mm) is about 23% greater than the thickness of the thermal boundary layer (λ_{th}= 1.3 mm) when the maximum reversal rate is observed [Fig. 4a]. In the following argument, we attempt to explain this mismatch and show that the heat blocking effect is most effective when λ_{th} is somewhat smaller than the sphere radius.

Nylon spheres have nearly the same heat diffusivity as the surrounding fluid. For an individual sphere, the vertical heat flux has to pass through both the solid sphere (thickness of order $d/2$) and a thermal boundary layer (thickness of order λ_{th}) that covers on the top of the sphere. The contrast between the heat fluxes with (j) and without (j_0) the spheres can be characterized by number $C = (j_0 - j)/j_0 = d/(2\lambda_{\mathrm{th}} + d)$, which ranges from 0 to 1 as for no heat flux blocking effect to ideal blocking. The effective thermal blanketing factor, Θ, is the combination (product) of the vertical heat contrast C and the area fraction Γ taken by the spheres, and $\Theta = C\Gamma = 4\lambda_{\mathrm{th}}(d-\lambda_{\mathrm{th}})/d(2\lambda_{\mathrm{th}}+d)$. When $\lambda_{\mathrm{th}} = d(\sqrt{3}-1)$= 1.2mm, factor Θ takes its maximum value and the heat blocking effect is most efficient. This number is now more consistent with our experimental observation.

The above simple argument has not taken into account of the complicated sphere geometry and the detailed packing patterns, which can only serve as a guide to better understand the thermal blanketing effects introduced by the spheres.

Moreover, the number of spheres also affects the reversal rate; it is greatest when the spheres are able to cover about half of the bottom plate (Fig. 4b). At this coverage, the spheres can create the highest contrast in heat flux at the bottom. With either a smaller or greater number of spheres, the bottom becomes geometrically more homogeneous and the heat contrast is reduced. Further, with more spheres present in the system, the suppressed mobility of spheres due to crowding also leads to longer reversal interval.

We have shown that a self-sustained, reorganizing state emerges as large-scale feedback (between many bodies and the surrounding fluid) overrides chaotic features intrinsic to a complex system. It is surprising that the freely-moving bodies introduced here do not destroy the existing coherent fluid structures, nor do they elicit more complex patterns in the system, but rather they provoke frequent switching between the two circulatory states. These free bodies, to some degree, are organized cyclically through passive response to the fluid; indeed, the collection of many bodies in our experiment behaves as a single deformable mass. We expect yet richer dynamics to occur if a similar study is conducted in cells with greater aspect ratios, where several large-scale circulation regions and dynamical states may co-exist.

We thank A. Libchaber, M. Shelley, S. Spagnolie, T. Bringley, J. Percus and J.-Q. Zhong for helpful discussions. This work is supported in part by the Department of Energy (Grant No. DE-FG0288ER25053).

---

* Electronic address: `jun@cims.nyu.edu`

[1] W. V. R. Malkus, Proc. R. Soc. London, Ser. A **225**, 185 (1954).
[2] R. Krishnamurti and L. N. Howard, Proc. Natl. Acad. Sci. **78**, 1981 (1981).
[3] M. Sano, X.-Z. Wu and A. Libchaber, Phys. Rev. A **40**, 6421 (1989).
[4] B. Castaing *et. al.*, J. Fluid Mech. **204**, 1 (1989).
[5] S. Ciliberto, S. Cioni and C. Laroche, Phys. Rev. E **54**, R5901 (1996).
[6] X.-L. Qiu and P. Tong, Phys. Rev. E **64**, 036304 (2001).
[7] Y. Tsuji, T. Mizuno, T. Mashiko and M. Sano, Phys. Rev. Lett. **94**, 034501 (2005).
[8] Lord Rayleigh, Philos, Mag. **32**, 529 (1916).
[9] T. Hartlep, A. Tilgner and F. H. Busse, Phys. Rev. Lett. **91**, 064501 (2003).
[10] S. Grossmann and D. Lohse, J. Fluid Mech. **407**, 27 (2000).
[11] S. Grossmann and D. Lohse, Phys. Rev. Lett. **86**, 3316 (2001).
[12] S. Ashkenazi and V. Steinberg, Phys. Rev. Lett. **83**, 3641 (1999).
[13] L. P. Kadanoff, Phys. Today **54**, 34 (2001).
[14] M. C. Cross and P. C. Hohenberg, Rev. Mod. Phys. **65**, 851 (1993).
[15] J. Maurer and A. Libchaber, J. Phys. (Paris), Lett. **41**, L515 (1980).
[16] M. H. Jensen, L. P. Kadanoff, A. Libchaber, I. Procaccia and J. Stavans, Phys. Rev. Lett. **55**, 2798 (1985).
[17] J. J. Niemela, L. Skrbek, K. R. Sreenivasan and R. J. Donnelly, Nature **404**, 837 (2000).
[18] J. A. Glazier, T. Segawa, A. Naert and M. Sano, Nature **398**, 307 (1999).
[19] E. Brown, A. Nikolaenko and G. Ahlers, Phys. Rev. Lett. **95**, 084503 (2005).
[20] H.-D. Xi, Q. Zhou and K.-Q. Xia, Phys. Rev. E **73** 056312 (2006).
[21] J. A. Whitehead, Phys. Earth Planet. Inter. **5**, 199 (1972).
[22] J. Zhang and A. Libchaber, Phys. Rev. Lett. **84**, 4361(2000).
[23] E. N. Popova and P. G. Frik, Fluid Dynamics **38**, 862 (2003).
[24] J.-Q. Zhong and J. Zhang, Phys. Fluids, **17**, 115105 (2005).
[25] K. R. Sreenivasan, A. Bershadskii and J. J. Niemela, Phys. Rev. E **65**, 056306 (2002).
[26] F. H. Busse, Geophys. J. R. Astron. Soc. **52**, 1 (1978).
[27] C. Grigné and S. Labrosse, Geophys. Res. Lett. **28**, 2707 (2001).
[28] A. Belmonte, A. Tilgner and A. Libchaber, Phys. Rev. Lett. **70**, 4067 (1993).
[29] H. L. Hinrichsen, J. Feder and T. Jøssang, Phys. Rev. A **41**, 4199 (1990).